Neuro 2004

P2-216 Analysis of mutated GFAP dynamics

Kenji Tanaka[1], Hirohide Takebayashi[1], Kazuhiro Ikenaka[1]
[1]Div. Neurobiol. Bioinfo., Natl. Inst. Physiol. Sci., Okazaki, Japan

Alexander disease is a falal neurological disorder caused by heterozygous mutation in GFAP. The pathological hallmark is the presence of astrocytic inclusion body called Rosenthal fibers, which contain GFAP. To understand the pathophysiology of this disease and utilize those results to the understanding of normal astrocytic function in vivo, we studied the dynamics of mutated GFAP in culture. We expressed wild type or mutated human GFAP gene in mouse primary astrocytes using adenoviral vectors and detected them using anti human GFAP specific antibody. Wild type GFAP formed normal appearing filaments with thick bundles or fascicular aggregations, whereas mutant GFAP did not form the fibrous structure but occasionally formed bulging bodies. When the cells expressing mutant GFAP were treated with proteasome inhibitor, the number of the cells harboring bulging bodies increased. These findings suggest that 1) mutant GFAP is incapable of forming the filament, 2) the formation of inclusion body caused by mutant GFAP is dependent on the proteosomal activity.

POSTER NO: 262

Towards delineation of the pathogenesis for juvenile recessive motor neuron diseases: Generation and characterization of the Als2 knockout mice

[1]Shinji Hadano, [2]Shigeru Kakuta, [2]Katsuko Sudo, [1]Asako Otomo, [1]Ryota Kunita, [1]Hikaru Mizumura, [1]Kyoko Suzuki, [2]Yoichiro Iwakura, [1]Joh-E Ikeda

[1]*SORST, Japan Science and Technology Corporation, and Department of Molecular Neuroscience, The Institute of Medical Sciences, Tokai University, Kanagawa 259-1193, Japan,* [2]*Center for Experimental Medicine, Institute of Medical Science, University of Tokyo, Tokyo 108-8639, Japan*

Recently, we and other groups have discovered the loss-of-functional mutations in the *ALS2* gene, accounting for a number of juvenile recessive motor neuron diseases (MNDs) including a type of juvenile ALS (ALS2), juvenile-onset PLS (PLSJ), and infantile-onset ascending hereditary spastic paralysis (IAHSP). The *ALS2* gene encodes a novel 184 kD protein, termed ALS2 or alsin, comprising three predicted guanine-nucleotide exchange factor (GEF) domains (RLD, DH/PH, and VPS9).

Most recently, we have demonstrated that the ALS2 protein specifically binds to Rab5 small GTPase and functions as a GEF for Rab5. Transiently expressed ALS2 localized to early endosomal compartments and stimulated endosome fusions through the activation of endogenous Rab5. This ALS2-associated Rab5GEF activity resides in the C-terminal region containing the MORN/VPS9 domain of ALS2. Further, the DH/PH domain strongly enhanced the VPS9 domain-mediated endosome fusions and stabilized its endosome localization. Based upon these findings, we propose that a perturbation of endosomal dynamics caused by loss of the ALS2-associated Rab5-GEF activity might underlie neuronal dysfunction and degeneration in ALS2/PLSJ/IAHSP. However, whether loss-of functional mutations in *ALS2* are sufficient to cause degeneration of motor neurons *in vivo* is still unknown. To address this issue, we sought to create a mouse model for the juvenile MND.

We generated mice homozygous for disruption of exon 3 of the mouse *Als2* gene by a standard homologous recombination strategy. Disruption of the *Als2* gene and null expression of the ALS2 protein were confirmed by PCR/southern blotting and western blotting analyses, respectively. The *Als2* knockout mice were born and grew with no obvious developmental as well as reproductive abnormalities by 7 months of age. Currently, behavioral and pathological analyses of these mice are underway. Generation of the *Als2* knockout mice should provide useful additional tools and clues to the understanding of the molecular pathogenesis for MNDs caused by the *ALS2* mutation.

POSTER NO: 269

The analysis of molecular function of nuclear-cytoplasm shuttling proteins, SLC2A4 and ZNF395, which bind to the novel cis-regulatory element in the human HD gene promoter

[1]Kazunori Tanaka, [1]Junko Shouguchi-Miyata, [2]Natsuki Miyamoto, [1]Joh-E Ikeda
[1]*The Institute of Medical Sciences, Tokai University, Isehara, Kanagawa 259-1193, Japan,* [2]*The Soluion Oriented Research for Science and Technology, Japan Science and Technology Corporation, Isehara, Kanagawa 259-1193, Japan*

Huntington's disease (HD) is a neurodegenerative disease caused by a CAG repeat expansion in exon 1 of the HD gene. The study of the conditional HD mouse gave a new aspect of the HD pathogenesis by means of perpetual expression of the mutated HD gene that might be a major causative for HD, and imply that HD is a reversible neurodegenerative disorder. However, molecular base of the transcriptional regulation of the HD gene in neurons has not been understood as yet.

To delineate the transcriptional regulation for the HD gene, we identified two members of a novel protein family, SLC2A4 and ZNF395, which bind to the promoter region for the HD gene using a yeast one-hybrid system. Amino acid sequence analysis of the proteins revealed that they shared similar domains, such as nuclear localization signal (NLS), nuclear export signal (NES), zinc-finger, and highly conserved C-terminal region. The study of subcellular distribution of ectopically expressed GFP-fused SLC2A4 and ZNF395 revealed the cytoplasmic localizations of both proteins, which were totally shifted from cytoplasm to nucleus through a NLS/NES-mediated pathway in either neuronal cell (IMR32) or non-neuronal cell (HeLa) lines. In vitro DNA binding and DNaseI protection assays indicated that the C-terminal conserved regions of both proteins were responsible for binding to the unique 7-bp consensus sequence (GCCGGCG) which resides in triplicate at intervals of 13bp within and proximal to the 20bp direct repeat sequences of the HD promoter region. Interestingly, reporter gene assays in conjunction with mutagenesis of the promoter sequences demonstrated that the 7-bp consensus sequence was essential for the HD promoter activity in a neuronal cell line, IMR32 cells, but not in HeLa cells.

Our study suggests that SLC2A4 and ZNF395 are novel transcription factors shuttling between nucleus and cytoplasm and bind to the specific GCCGGCG, which is an essential cis-element for the HD gene expression in neuronal cells.

207

The DH/PH domain of ALS2 strongly enhances the C-terminal MORN/VPS9 domain-mediated endosome fusions

Ryota Kunita[1], Shinji Hadano[1,2], Asako Otomo[2], Hikaru Mizumura[1], Takeya Okada[2], Kyoko Suzuki[2], Shuh Narumiya[3], and Joh-E Ikeda[1,2,4]
[1]SORST, JST, [2]IMS, Tokai Univ., [3]Dept. Pharmacol., Kyoto Univ., [4]Dept. Paediatrics, Univ. Ottawa

We have identified *ALS2* as a causative gene for a juvenile recessive form of amyotrophic lateral sclerosis (ALS2; OMIM205100) [*Nat. Genet.*, (2001) **29**, 166-173]. The *ALS2* gene encodes a 184-kD protein, termed ALS2, containing three putative guanine nucleotide exchange factor (GEF) domains [RCC1-like domain (RLD), DH/PH, and VPS9] and MORN motifs. Recently, we have demonstrated that ALS2 specifically binds to Rab5 and functions as a GEF on Rab5. Transiently expressed ALS2 localizes to early endosomal compartments and stimulates endosome fusions through the activation of endogenous Rab5. Further, this ALS2rab5GEF activity resides in the ALS2 C-terminal region containing the MORN/VPS9 domain [*Hum. Mol. Genet.*, (2003) **12**, 1671-1687]. Here we show a novel function of the DH/PH domain, which strengthens the function of the MORN/VPS9 domain. We analyzed HeLa cells transiently expressing a series of ALS2 mutants carrying a deletion and/or substitution, and found that, in the context of the C-terminal half of the ALS2 peptide comprising DH/PH/MORN/VPS9, the DH/PH domain strongly enhanced the MORN/VPS9 domain-mediated endosome fusions and stabilized endosome localization of the C-terminal ALS2 peptide. A partial deletion or substitution in either DH or PH domain resulted in complete loss of the enhancing effect of endosome fusions as well as correct targeting of the ALS2 protein onto endosomal compartments, indicating that both DH and PH are necessary for both of these functions. On the other hand, expression of the ALS2 C-terminal peptides carrying Rab5GEF defective mutations in the VPS9 domain obliterated the enlarged-endosome phenotypes, demonstrating that the enhancement of the endosomal fusions by the DH/PH domain relies on the ALS2rab5GEF activity. Taken together, these results suggest that the DH/PH domain act to target ALS2 onto endosomal compartments, thereby leading to the persistent upregulation of MORN/VPS9-mediated Rab5 activation and endosome fusions.

215 **Amyotrophic lateral sclerosis type 2 gene encodes protein, ALS2, is a novel guanine nucleotide exchange factor for Rab5 and implicates in endosomal dynamics**

Asako Otomo[1,2], Shinji Hadano[1,2], Takeya Okada[2],
Hikaru Mizumura[1], Ryota Kunita[1], Hitoshi Nishijima[3],
Junko Showguchi-Miyata[2], Yoshiko Yanagisawa[1],
Eri Kohiki[1], Etsuko Suga[1], Masanori Yasuda[4],
Hitoshi Osuga[1,2],Takeharu Nishimoto[3], Shuh Narumiya[5]
& Joh-E Ikeda[1,2,6]
[1]SORST, JST, Tokai Univ, Japan. [2]IMS, Tokai Univ. Japan. [3]Grad of Med Sci, Kyushu Univ, Japan. [4]Dept of Pathol, Fac Med, Tokai Univ, Japan.[5]Grad of Med Sci, Kyoto Univ, Japan. [6]Fac of Med, Univ of Ottawa, Canada.

ALS2 was initially identified as a causative gene for a juvenile recessive form of amyotrophic lateral sclerosis (ALS), termed ALS2 (OMIM 205100). *ALS2* mutations account for a number of recessive motor neuron diseases including forms of ALS, PLSJ, and HSP. ALS2 is a 184-kD protein comprising several putative guanine nucleotide exchange factor (GEF) domains [RLD; RCC1 like domain, DH.PH domain, VPS9; Vacuolar protein sorting 9 domain] and motifs, but the functions of the ALS2 protein have not been revealed as yet. To delineate the functions of the ALS2 protein, biochemical and cell biological analyses were employed in this study. We demonstrate that the ALS2 protein specifically binds to the small GTPase Rab5 and functions as a GEF for Rab5, ALS2rab5GEF. In addition, the ectopically expressed carboxy-terminal ALS2 peptide and Rab5A colocalized to early endosomes, consistent with the ALS2 protein involvement in endosomal trafficking and fusion in conjunction with the activation of Rab5. These results imply that an obstruction of endosomal dynamics might underlie neuronal dysfunction and degeneration in ALS2 as well as PLSJ and HSP for which *ALS2* mutations account.

PAPER

Multiple regional ^{1}H-MR spectroscopy in multiple system atrophy: NAA/Cr reduction in pontine base as a valuable diagnostic marker

H Watanabe, H Fukatsu, M Katsuno, M Sugiura, K Hamada, Y Okada, M Hirayama, T Ishigaki, G Sobue

J Neurol Neurosurg Psychiatry 2004;75:103–109

See end of article for authors' affiliations

Correspondence to: Gen Sobue, MD, Department of Neurology, Nagoya University Graduate School of Medicine, Nagoya 466-8550 Japan; sobueg@med.nagoya-u.ac.jp

Received 20 December 2002
In revised form 31 March 2003
Accepted 17 May 2003

Objective: We performed ^{1}H-MR spectroscopy (^{1}H-MRS) on multiple brain regions to determine the metabolite pattern and diagnostic utility of ^{1}H-MRS in multiple system atrophy (MSA).
Methods: Examining single voxels at 3.0 T, we studied metabolic findings of the putamen, pontine base, and cerebral white matter in 24 MSA patients (predominant cerebellar ataxia (MSA-C), n=13), parkinsonism (MSA-P), n=11), in 11 age and duration matched Parkinson's disease patients (PD) and in 18 age matched control subjects.
Results: The *N*-acetylaspartate to creatine ratio (NAA/Cr) in MSA patients showed a significant reduction in the pontine base ($p<0.0001$) and putamen ($p=0.02$) compared with controls. NAA/Cr in cerebral white matter also tended to decline in long standing cases. NAA/Cr reduction in the pontine base was prominent in both MSA-P ($p<0.0001$) and MSA-C ($p<0.0001$), and putaminal NAA/Cr reduction was significant in MSA-P ($p=0.009$). It was also significant in patients who were in an early phase of their disease, and in those who showed no ataxic symptoms or parkinsonism, or did not show any MRI abnormality of the "hot cross bun" sign or hyperintense putaminal rims. NAA/Cr in MSA-P patients was significantly reduced in the pontine base ($p=0.001$) and putamen ($p=0.002$) compared with PD patients. The combined ^{1}H-MRS in the putamen and pontine base served to distinguish patients with MSA-P from PD more clearly.
Conclusions: ^{1}H-MRS showed widespread neuronal and axonal involvement in MSA. The NAA/Cr reduction in the pontine base proved highly informative in the early diagnosis of MSA prior to MRI changes and even before any clinical manifestation of symptoms.

Multiple system atrophy (MSA) is a sporadically occurring neurodegenerative disease that presents parkinsonism, cerebellar ataxia, autonomic failure, and pyramidal signs of varying severity during the course of illness.[1–3] Neuropathological findings consist of a varying neuronal loss, gliosis, and demyelination with widespread regional involvement, particularly including the striatonigral, olivopontocerebellar, and autonomic nervous systems.[4–6] The tempo and progression of multiple system involvement vary widely among individual MSA patients and have been closely related to both functional deterioration and prognosis by clinical evaluation.[7] Thus, assessing the multi-regional involvement in MSA is essential for accurate diagnosis, counselling of patients and families, optimal management of symptoms, and the usefulness of future therapeutic trials.

Proton magnetic resonance spectroscopy (^{1}H-MRS) is a valuable non-invasive MR technique for monitoring brain metabolism in vivo.[8–18] The major peaks of the ^{1}H-MRS spectrum, corresponding to *N*-acetylaspartate (NAA), creatine (Cr), and choline (Cho) containing phospholipids, have been used to evaluate neuronal loss and active myelin breakdown. The ratio of NAA to Cr (NAA/Cr) is considered a metabolic marker reflecting the functional status of neurones and axons in the brain, with a decrease indicating neuronal or axonal loss or dysfunction. Previous studies using ^{1}H-MRS in MSA with predominant parkinsonism (MSA-P) reported a significant NAA/Cr reduction in the striatum compared with Parkinson's disease (PD) patients and normal subjects.[11–14] However, the pontine base and cerebral white matter, which are also pathologically involved in MSA, have not been fully assessed by ^{1}H-MRS. Recent technical innovations have permitted ^{1}H-MRS at higher magnetic field strengths.[19–21] Multi-regional data can be obtained from single voxel ^{1}H-MRS within a short examination time with increasing signal to noise ratio (SNR).

Our purpose was to assess the extent of multiple system involvement in patients with MSA by using multiple regional single voxel ^{1}H-MRS including the putamen, pontine base, and cerebral white matter (CWM), and to further assess the diagnostic value of the regional ^{1}H-MRS.

METHODS

All patients and control subjects gave written informed consent. The MR protocol was approved by the Ethics Committee of the Nagoya University School of Medicine. Twenty four patients with MSA (12M, 12F; mean (SD) age 61 (7) years old), 11 patients with PD (5M, 6F; 63 (9) years old), and 18 control subjects with no history of any neurological disease (10M, 8F; 59 (7) years old) were studied. No significant differences in male to female ratio or age were noted among the three groups. The duration from initial

Abbreviations: Cho, choline; Cr, creatine; CWM, cerebral white matter; HCB, "hot cross bun"; HPR, hyperintense rim; MRI, magnetic resonance imaging; MRS, magnetic resonance spectroscopy; MSA, multiple system atrophy; MSA-C, multiple system atrophy with cerebellar ataxia predominant; MSA-P, multiple system atrophy with parkinsonism predominant; NAA, *N*-acetylaspartate; PD, Parkinson's disease; SNR, signal to noise ratio; VOI, volume of interest.

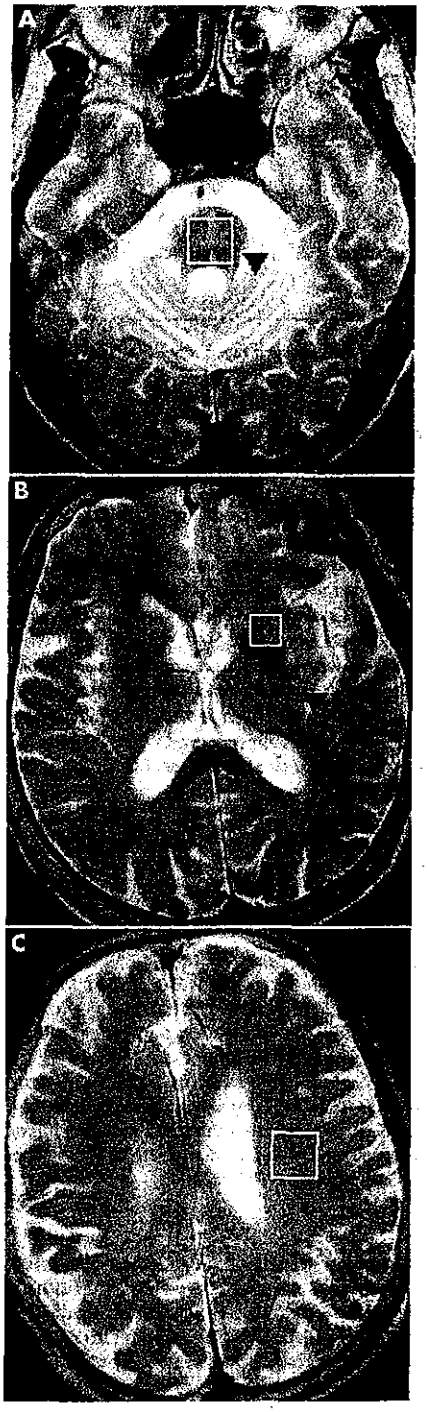

Figure 1 Location of volumes of interest are shown by squares in the pontine base (A), putamen (B), and white matter of the frontal lobe (C). Additionally, in these images, an HCB sign is present in the pons (A), as is a hyperintense putaminal rim (B). Axial T2 weighted images (3.0 T; TR: 3970, TE: 80), with respective findings are indicated by arrowheads.

symptoms to MRI and MRS evaluation also showed no differences between MSA and PD patients (MSA; 3.7 (2.4) years; PD; 4.4 (2.2) years, $p>0.4$). Diagnoses of all MSA and PD patients were "probable" according to established diagnostic criteria.[3 22] As for subtypes of MSA, cerebellar dysfunction (MSA-C) predominated in 13 patients and parkinsonism (MSA-P) in 11. We classified patients into two groups according to the presence of parkinsonian signs in MSA, based on the consensus statement for MSA diagnosis. Patients with bradykinesia plus at least one sign of either rigidity, postural instability, or tremor were considered to manifest parkinsonism and designated as "parkinsonism+", while others were taken to be "parkinsonism−". As for cerebellar dysfunction, patients with gait ataxia plus at least one sign of ataxic dysarthria, limb ataxia, or sustained gaze evoked nystagmus were considered "ataxia+", and others as "ataxia−" based on the consensus criteria.[3] Six of nine MSA-P patients and all PD patients were taking medication for parkinsonism (benserazide/levodopa 25/100 mg, or carbidopa/levodopa 10/100 mg, two or three times daily). All PD patients showed a good response to treatment.

MRI and ^{1}H-MRS were performed with a 3.0 T system (Bruker, Ettlingen, Germany) using a standard head coil with circular polarisation. The imaging protocol consisted of sagittal T1 weighted spin echo sequences (repetition time (TR), 460 ms; echo time (TE), 14 ms) and transverse T2 weighted sequences (TR, 3970 ms; TE, 80 ms). Slice thickness was 6 mm with a 1.2 mm gap and a 512×384 matrix. We evaluated whether a "hot cross bun" (HCB) sign was present in the pons and whether the putamen showed a hyperintense rim (HPR), according to the criteria described in previous reports (fig 1A; B).[7 23–26] The spectroscopic volume of interest (VOI) was placed in the pontine base (2.2 to 3.4 cm^3), the putamen (1 cm^3), and the CWM (3.4 cm^3; fig 1A to C). Voxel size was chosen to be as small as possible while maintaining an acceptable SNR in order to minimise the partial volume effect. Care was taken not to incorporate cerebrospinal fluid spaces within a VOI. The VOI in the putamen was placed on the more affected side, and the frontal lobe VOI was ipsilateral to the putaminal VOI. ^{1}H-MR spectra were acquired using a point resolved spectroscopy sequence with chemical shift selective water suppression. Spectral parameters were as follows: TR: 2000 ms; TE: 30 ms; averages: 256 in the putamen, and 64 each in the centrum semiovale and pons; data points: 1024. A shimming procedure focused on the water signal was performed to obtain a uniform and homogenous magnetic field. After Fourier transformation and zero order phase correction, relative metabolite concentrations for NAA at 2.0 ppm, Cr at 3.0 ppm, and Cho at 3.2 ppm were determined by Lorentzian curve fitting of the corresponding resonance in the frequency spectra. The baseline was corrected for purposes of data presentation. From these data, the metabolite ratios NAA/Cr, and Cho/Cr were determined as semiquantitative values. Post-procedural processing was performed by the same radiologist (HF). All preconditioning, spectroscopic measurements, and processing were performed with Paravision 2.01 software (Bruker). Total examination time including MRI and ^{1}H-MRS was <1 hour. One MSA-C patient with severe pontine atrophy was excluded because a good pontine spectrum could not be obtained.

Values obtained were entered into a database for further statistical analysis. The Mann-Whitney U test and the Kruskal-Wallis test for nonparametric statistics were performed as appropriate. When the Kruskal-Wallis test indicated differences among groups, in a multiple comparison analysis, Scheffé's test was used to identify which group differences accounted for the significant p value. Relationships of NAA/Cr reduction to duration of illness were analysed using Pearson's correlation coefficient. Calculations were performed using the Stat View statistical software package (Abacus Concepts, Berkeley, CA, USA). Statistical significance was defined as $p<0.05$.

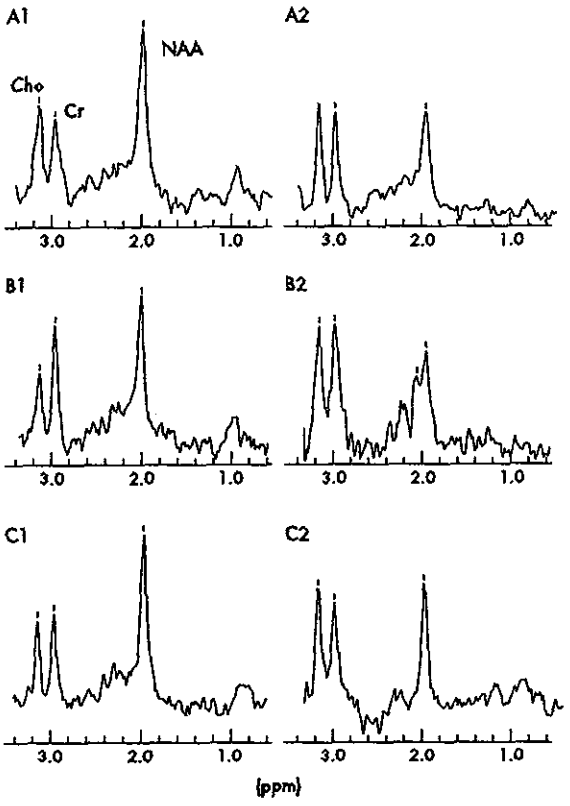

Figure 2 Representative ^{1}H-MRS spectra from control and MSA subjects. A1, B1, and C1 represent spectra from a control subject's pontine base, putamen, and cerebral white matter, respectively. A2, B2, and C2 represent spectra from those same three regions in an MSA patient. NAA, *N*-acetylaspartate; Cho, choline; Cr, creatine; MSA, multiple system atrophy; CWM, cerebral white matter.

RESULTS

Widespread NAA/Cr reduction in MSA in multiple regional ^{1}H-MRS

A representative MSA patient (fig 2) showed a marked reduction of the NAA peak in the pontine base, putamen, and cerebral white matter compared with controls. NAA/Cr was significantly reduced in the pontine base of MSA patients ($p<0.0001$) and in the putamen ($p = 0.02$) compared with controls. MSA patients also showed a lower NAA/Cr in cerebral white matter than controls, but this difference was not statistically significant ($p = 0.12$). Cho/Cr was only slightly increased in MSA, and no significant differences were found among the three groups for the pontine base, putamen, and CWM.

Prominent NAA/Cr reduction in pontine base in both MSA-C and MSA-P

Significant reductions of NAA/Cr were evident in the pontine base, putamen, and CWM in MSA-C and MSA-P compared with controls (fig 3A–C). MSA-C patients showed a significant reduction of NAA/Cr in the pontine base ($p<0.0001$) and CWM ($p = 0.02$), but not in the putamen. MSA-P patients showed a significant reduction of NAA/Cr in the pontine base ($p<0.0001$) and putamen ($p = 0.009$) but not in the CWM. These observations indicate that the NAA/Cr reduction in the pontine base was significant in both MSA-C and MSA-P. Cho/Cr was not changed in MSA-P or MSA-C compared with controls.

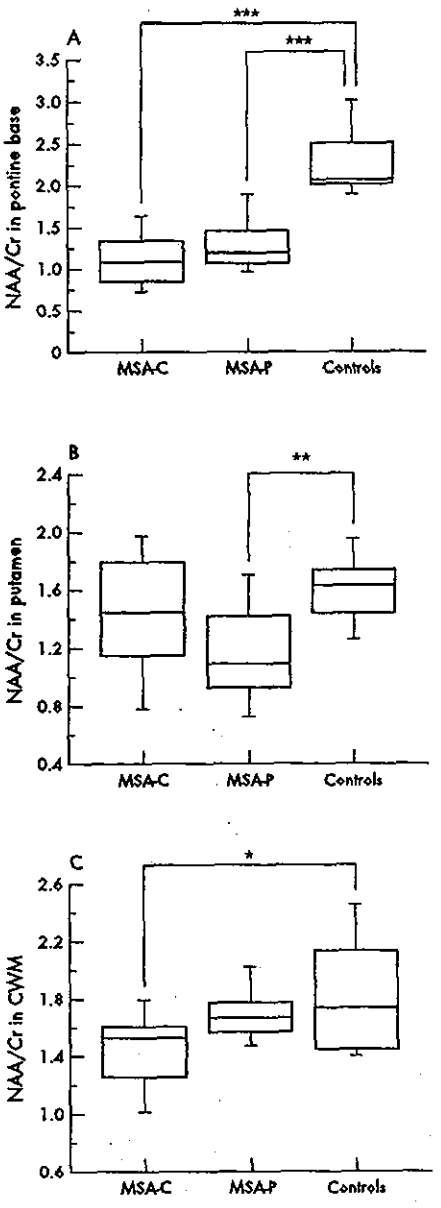

Figure 3 Box and whisker plot of the NAA/Cr ratio. Horizontal lines indicate median values. Boxes extend from the 25th to the 75th percentile. A, B, and C respectively show NAA/Cr in the pontine base, putamen, and cerebral white matter, comparing MSA-C, MSA-P, and control subjects. *$p = 0.02$, **$p = 0.009$, and ***$p<0.0001$ by Scheffé's test, respectively. NAA, *N*-acetylaspartate; Cr, creatine; Cho, choline containing component; MSA-C, multiple system atrophy with cerebellar ataxia predominant; MSA-P, multiple system atrophy with parkinsonism predominant.

Relation of NAA/Cr reduction in pontine base with disease phase, motor symptoms and MRI abnormalities in MSA

In terms of disease duration, the NAA/Cr reduction was most significant in the pontine base of patients with MSA even in an early phase of illness (fig 4). A tendency toward an inverse

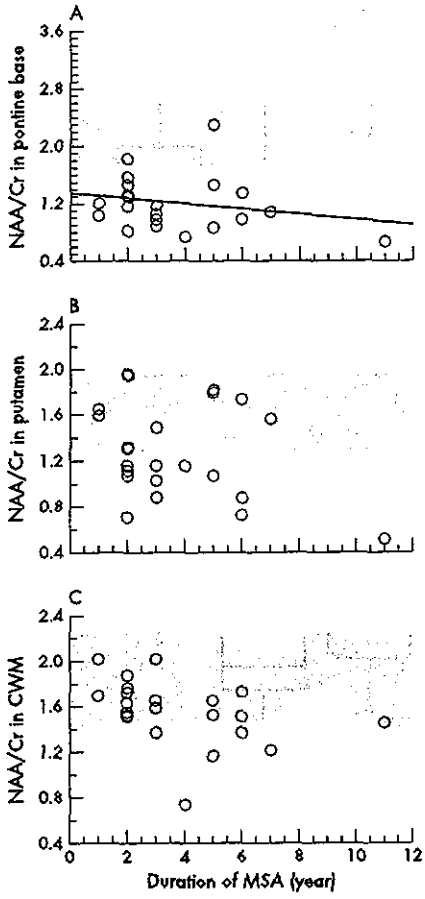

Figure 4 Correlation with duration of MSA of individual NAA/Cr ratios in the pontine base (A), putamen (B), and cerebral white matter (C). The shaded area corresponds to the mean (SD) of NAA/Cr in control subjects. NAA, N-acetylaspartate; Cr, creatine; CWM, cerebral white matter; MSA, multiple system atrophy.

relationship between disease duration and NAA/Cr in the three regions was observed, but did not attain significance (pontine base: $r = -0.24$, $p = 0.29$; putamen: $r = -0.32$, $p = 0.14$; CWM: $r = -0.41$, $p = 0.06$). NAA/Cr in the pontine base was significantly reduced compared with controls even in patients who did not show ataxic symptoms ($p = 0.0006$, fig 5A-1). However, NAA/Cr in the putamen and white matter was not reduced in patients with ataxia (fig 5B-1, C-1). NAA/Cr in the putamen was markedly decreased in MSA patients with parkinsonism ($p = 0.02$, Fig 5B-2), whereas patients without it exhibited no significant reduction compared with controls. NAA/Cr reduction in the pontine base, on the other hand, was significant ($p<0.0001$) irrespective of parkinsonism (Fig 5A-2).

The MRI revealed the HCB sign in the pontine base in eleven MSA patients (46%) and the HPR sign in six (25%). A significant reduction of NAA/Cr was seen in the pontine base even in patients without ($p<0.0001$) as well as in those with an HCB sign ($p<0.0001$; fig 5A-3). In the putamen and cerebral white matter, NAA/Cr values did not show any significant difference irrespective of the HCB sign (fig 5B-3, C-3). Moreover, NAA/Cr significantly decreased in the pontine base in patients both with and without HPR (fig 5A-4). NAA/Cr in the putamen and cerebral white matter did not show any significant differences irrespective of HPR signs (fig 5B-4, C-4). Cho/Cr had no significant relationship to ataxic, parkinsonism, or MRI abnormalities.

NAA/Cr in pontine base in MSA-P and PD

NAA/Cr reduction in the pontine base was highly significant in patients with MSA-P compared with both controls and PD ($p<0.0001$, $p = 0.001$; fig 6A). NAA/Cr in the putamen in MSA-P patients also showed a significant decrease compared with both controls and PD ($p = 0.003$, $p = 0.002$; fig 6B). No significant differences in NAA/Cr were noted in cerebral white matter between MSA-P and PD. These data indicate that the NAA/Cr reduction in the pontine base is a valuable marker to discriminate MSA-P from PD. In addition, combining individual NAA/Cr values for the pontine base and putamen further reduced the overlap between MSA-P and PD (fig 6D), suggesting that a combined assessment of the pontine base and putamen was more effective in discriminating between MSA-P and PD than individual area assessments. Cho/Cr did not display any significant changes in the pontine base, putamen or cerebral white matter.

DISCUSSION

We demonstrated widespread NAA/Cr reduction in the pontine base, putamen and in some cases, in the cerebral hemisphere, but no significant Cho/Cr alteration in patients with MSA using localised ^{1}H-MRS at 3.0 T. In this study, absolute metabolite concentrations were not measured. However, the specific conditions that may change the total Cr signal, such as trauma, hyperosmolar conditions, hypoxia, stroke, and tumours, were not included. Age was matched among MSA, PD, and control groups. Moreover, quantitative studies did not show significant Cr changes between MSA patients and control subjects.[11 16] Thus, the reduction of the NAA/Cr ratio in the present study can be considered due to a selective decrease in NAA levels.

NAA has been immunohistochemically demonstrated to localise almost exclusively within neurones and axons,[27 28] but some in vitro studies have also detected NAA expression in mature, immature, and undifferentiated oligodendrocytes.[29 30] Nevertheless, according to a recent study, in vivo MRS measurements of NAA remain axon specific, with no oligodendrocytes, nonproliferating oligodendrocyte progenitor cells, or myelin contributing to detectable NAA in the mature CNS.[31] This result supports the view that the widespread NAA/Cr reductions observed in this study ultimately reflect widespread neuronal and axonal involvement in MSA, although oligodendrocytes might influence the NAA levels to some degree.

The striking observation in this study is that the NAA/Cr reduction in the pontine base was the most significant among the three regions examined. That reduction was detected in the early phase of illness even in patients with no symptoms of ataxia or parkinsonism, or in patients without MRI abnormality of the HCB sign. Moreover, the pontine NAA/Cr reduction was significant even in MSA-P patients. In addition, NAA/Cr reductions in the pontine base were seen even in patients with no HPR sign in the lateral putamen. These observations suggest that NAA/Cr reduction in the pontine base is an accurate diagnostic marker for MSA even in patients in an early stage and a pre-symptomatic phase of ataxia or parkinsonism. The diagnostic focus of ^{1}H-MRS in MSA has been on the putamen,[11–14] whereas our results unequivocally demonstrated that MRS abnormality can be detected sooner and more universally in the pontine base than in the putamen in the course of the disease. The question is why a significant NAA/Cr reduction can be detected more readily in the pontine base than in the putamen. One reason may be that neuroaxonal degeneration

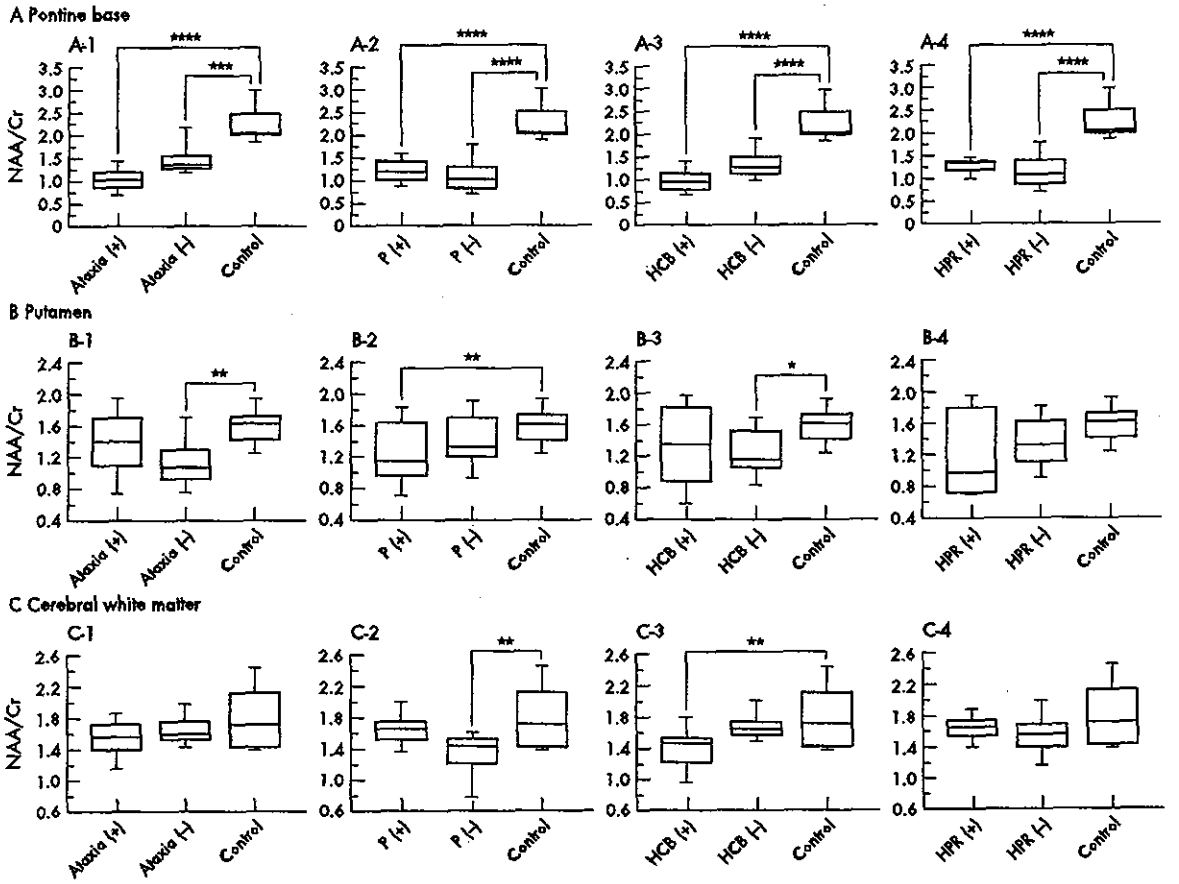

Figure 5 NAA/Cr in the pontine base (A), putamen (B) , and cerebral white matter (C) for MSA patients classified in terms of clinical features of ataxia (+ or −; A-1, B-1, C-1), parkinsonism (P; + or −; A-2, B-2, C-2), HCB on MRI (+ or −; A-3, B-3, C-3), and hyperintense putaminal rim (HPR) on MRI (+ or −; A-4, B-4, C-4). +, Presence; −, absence. *p=0.047, **p=0.02, ***p=0.0006, and ****p<0.0001 by Scheffé's test, respectively. NAA, *N*-acetylaspartate; Cr, creatine; MSA, multiple system atrophy; CWM, cerebral white matter.

in the pons would be more extensive than in the putamen. As the pontine base consists of the axons and neurones specifically involved in MSA (for example fibres of cerebellar inflow and outflow, corticospinal tracts and transverse pontine tracts), subclinical involvement of such fibres could be detected as a reduction of NAA/Cr. Furthermore, because, as we demonstrated previously, MSA-C is significantly more prevalent in Japan than MSA-P, compared with white populations in the western countries,[7] the cerebellar pontine system should be more profoundly involved in Japanese MSA patients. A second possibility is that the volume effect due to putaminal atrophy would ultimately include the neighbouring normal tissues in the VOI of the MRS, influencing the degree of the NAA/Cr reduction. As atrophy of the putamen is severe in certain patients, the size of the VOI is a limiting factor in ^{1}H-MRS for maintaining an acceptable SNR. Such volume effects due to putaminal atrophy can result in conflicting data. Clarke and Lowry reported an absence of significant reductions in basal ganglionic NAA/Cr in MSA,[16] precluding the use of NAA/Cr reductions in the striatum for differential diagnosis.[18] Disease duration in their patients averaged 7.9 years.[16] In contrast, mean disease duration in other reports showing significant NAA/Cr reductions in the striatum of MSA patients ranged from 3.2 to 4.5 years,[11–14] similar to the duration in our patients. Because, with longer duration, putaminal atrophy in patients with MSA-P becomes more severe, discrepancies could be explained by differences in putaminal atrophy that can profoundly influence ^{1}H-MRS results. By avoiding this volume effect, MRS for the pontine base would provide a more accurate diagnostic marker.

Discriminating clearly between MSA-P and PD has long been a diagnostic problem from both therapeutic and prognostic viewpoints. Putaminal NAA/Cr reduction was significant in MSA-P patients compared with PD and control subjects, as previously reported.[11–14] However, as discussed above, the putaminal volume effect could influence the significance of putaminal NAA/Cr reduction, particularly in patients with advanced disease. Although brainstem and cerebellar involvement is an important and specific finding in differentiating MSA-P from PD,[26 32] the sensitivity of both clinical and MRI evaluations of these abnormalities is relatively low.[7 26] Based on our results, we believe that ^{1}H-MRS assessment of the pontine base would be of considerable value in the differential diagnosis between MSA-P and PD. However, combined ^{1}H-MRS study of the pontine base and putamen can provide a more sensitive differentiation between MSA-P and PD than a conventional single regional study, such as that of the putamen.

The cerebral hemisphere is involved more extensively in MSA than previously believed. Recently, Abe *et al* reported a significant decrease in NAA/Cr in MSA, involving Brodmann's areas 6, 8, and 46.[14] Moreover, Spargo *et al*

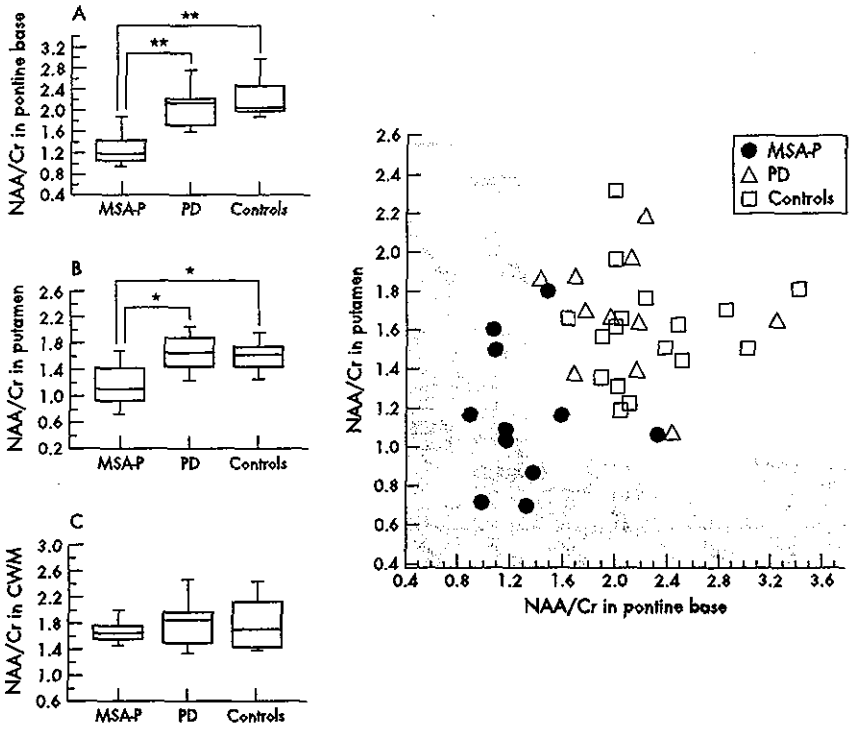

Figure 6 Box and whisker plot of the NAA/Cr ratio in the pontine base (A), putamen (B) and cerebral white matter (CWM, C) compared between MSA-P, PD, and controls. D is a scatter plot of the individual NAA/Cr data in the pontine base *v putamen including* MSA-P, PD, and control subjects. The scaled area corresponds to the *mean−2 SD of* NAA/Cr *in* the pontine base and putamen of control subjects. *p=0.002, **p<0.0001 by Scheffé's test, respectively. NAA, *N*-acetylaspartate; Cr, creatine; MSA-P, multiple system atrophy with parkinsonism predominant.

reported 18.7% and 21.4% neuronal loss in the primary and supplementary motor cortex, respectively.[35] In addition, the degree of atrophy in cerebral hemispheric areas varies between individuals, often becoming severe in long standing *cases.*[34] *We found a mild overall reduction of NAA/Cr in CWM* with a more significant NAA/Cr reduction in the subgroup with a longer duration of illness. This finding is in good agreement with previous ^{1}H-MRS reports and pathological observations.

Davie *et al*[11] reported a significant reduction of Cho/Cr ratio suggesting reduced membrane turnover in the lentiform nucleus in MSA, perhaps as result of cell loss. In the present study, Cho/Cr showed little change throughout the course of disease in the putamen, pontine base, and CWM, in agreement with other reports.[12–14 16] The relevance of this discrepancy *is uncertain. One possible explanation is the* difference of technical factors such as size of VOI and echo time. On the other hand, pathological study shows not only cell loss but also widely and variously distributed myelin degeneration in MSA brains that may increase the Cho.[35] Thus, heterogeneity of lesions in association with disease stage also may influence the Cho/Cr result. Further longitudinal studies and comparison of ^{1}H-MRS with histological *findings will be needed to clarify* the uncertainty as to the Cho/Cr ratio in MSA.

In conclusion, localised ^{1}H-MRS at 3.0 T in multiple regions showed widespread neuronal and axonal involvement in patients with MSA. NAA/Cr reduction in the pontine base provided a significant diagnostic marker for MSA irrespective of the disease form of MSA-P or MSA-C, disease duration, symptomatic manifestations, or MRI abnormalities. Moreover, combined ^{1}H-MRS study of the pontine base and putamen proved particularly effective in differentiating MSA from PD. We believe that ^{1}H-MRS would provide an early and accurate MSA diagnosis, an enhanced *understanding of its* pathogenetic mechanism, and the conclusiveness needed for future therapeutic trials.

Authors' affiliations
H Watanabe, M Katsuno, M Sugiura, K Hamada, Y Okada, M Hirayama, G Sobue, Department of Neurology, Nagoya University Graduate School of Medicine, Japan
H Fukatsu, T Ishigaki, Department of Radiology, Nagoya University Graduate School of Medicine, Japan

Competing interest: none declared

REFERENCES

1 **Graham JG**, Oppenheimer DR. Orthostatic hypotension and nicotine sensitivity in a case of multiple system atrophy. *J Neurol Neurosurg Psychiatry* 1969;32:28–34.
2 **Quinn N.** Multiple system atrophy–the nature of the beast. *J Neurol Neurosurg Psychiatry* 1989;52:78–89.
3 **Gilman S**, Low PA, Quinn N, *et al.* Consensus statement on the diagnosis of multiple system atrophy. *J Neurol Sci* 1999;163:94–8.
4 **Sobue G**, Terao S, Kachi T, *et al.* Somatic motor efferents in multiple system atrophy with autonomic failure: a clinico-pathological study. *J Neurol Sci* 1992;112:113–25.
5 **Wenning GK**, Ben-Shlomo Y, Magalhes M, *et al.* Clinicopathological study of 35 cases of multiple system atrophy. *J Neurol Neurosurg Psychiatry* 1995;58:160–6.
6 **Lantos P.** The definition of multiple system atrophy: A review of recent developments. *J Neuropathol Exp Neurol* 1998;57:1099–111.
7 **Watanabe H**, Saito Y, Terao S, *et al.* Progression and prognosis in multiple system atrophy; an analysis of 230 Japanese patients. *Brain* 2002;125:1070–83.
8 **Ross B**, Michaelis T. Clinical applications of magnetic resonance spectroscopy. *Magn Reson Q* 1994;10:191–247.
9 **Davie CA.** The role of spectroscopy in parkinsonism. *Mov Disord* 1998;13:2–4.
10 **Rudkin TM**, Arnold DL. Proton magnetic spectroscopy for the diagnosis and management of cerebral disorders. *Arch Neurol* 1999;56:919–26.
11 **Davie CA**, Wenning GK, Barker GJ, *et al.* Differentiation of multiple system atrophy from idiopathic Parkinson's disease using proton magnetic resonance spectroscopy. *Ann Neurol* 1995;37:204–10.
12 **Federico F**, Simone IL, Lucivero V, *et al.* Proton magnetic resonance spectroscopy in Parkinson's disease and atypical parkinsonian disorders. *Mov Disord* 1997;12:903–9.
13 **Federico F**, Simone IL, Lucivero V, *et al.* Usefulness of proton magnetic resonance spectroscopy in differentiating parkinsonian syndromes. *Ital J Neurol Sci* 1999;20:223–9.
14 **Abe K**, Terakawa H, Takanashi M, *et al.* Proton magnetic resonance spectroscopy of patients with parkinsonism. *Brain Res Bull* 2000;52:589–95.

15 **Terakawa H**, Abe K, Watanabe Y, *et al.* Proton magnetic resonance spectroscopy (1H MRS) in patients with sporadic cerebellar degeneration. *J Neuroimaging* 1999;**9**:72–7.
16 **Clarke CE**, Lowry M. Basal ganglia metabolite concentrations in idiopathic Parkinson's disease and multiple system atrophy measured by proton magnetic resonance spectroscopy. *Eur J Neurol* 2000;**7**:661–5.
17 **Hu MTM**, Simmons A, Glover A, *et al.* Proton magnetic resonance spectroscopy of the putamen in Parkinson's disease and multiple system atrophy. *Mov Disord* 1998;**13**:182.
18 **Clarke CE**, Lowry M. Systematic review of proton magnetic resonance spectroscopy of the striatum in parkinsonian syndromes. *Eur J Neurol* 2001;**8**:573–7.
19 **Bomsdorf H**, Helzel T, Kunz D, *et al.* Spectroscopy and imaging with a 4 Tesla whole-body MR system. *NMR Biomed* 1988;**1**:151–8.
20 **Hetherington HP**, Pan JW, Chu W-J, *et al.* Biological and clinical MRS at ultra-high field. *NMR Biomed* 1988;**10**:360–71.
21 **Gruetter R**, Weisdorf SA, Rajanayagan V, *et al.* Resolution improvements in vivo NMR spectra with increased magnetic field strength. *J Magn Reson* 1988;**135**:260–4.
22 **Calne DB**, Snow BJ, Lee C. Criteria for diagnosing Parkinson's disease. *Ann Neurol* 1992;**32**:S125–7.
23 **Savoiardo M**, Strada L, Girotti F, *et al.* Olivopontocerebellar atrophy: MR diagnosis and relationship to multiple system atrophy. *Radiology* 1990;**174**:693–6.
24 **Kraft E**, Schwarz J, Trenkwalder C, *et al.* The combination of hypointense and hyperintense signal changes on T2-weighted magnetic resonance imaging sequences: a specific marker of multiple system atrophy? *Arch Neurol* 1999;**56**:225–8.
25 **Konagaya M**, Sakai M, Matsuoka Y, *et al.* Pathological correlate of the slitlike changes on MRI at the putaminal margin in multiple system atrophy. *J Neurol* 1999;**246**:142–3.
26 **Schrag A**, Good CD, Miszkiel K, *et al.* Differentiation of atypical parkinsonian syndromes with routine MRI. *Neurology* 2000;**54**:697–02.
27 **Moffett JR**, Namboodiri MAA, Cangro CB, *et al.* Immunohistochemical localization of N-acethylaspartate in rat brain. *Neuroreport* 1991;**2**:131–4.
28 **Simmons ML**, Frondoza CG, Coyle JT. Immunohistochemical localization of N-acethylaspartate with monoclonal antibodies. *Neuroscience* 1991;**45**:37–45.
29 **Urenjak J**, Williams SR, Gadian DG, *et al.* Specific expression of N-acethylaspartate in neurons, oligodendrocyte type-2 astrocyte progenitors, and immature oligodendrocyte in vitro. *J Neurochem* 1992;**59**:55–61.
30 **Bhakoo KK**, Pearce D. In vivo expression of N-acetylaspartate by oligodendrocytes: implications for proton magnetic resonance spectroscopy signal in vivo. *J Neurochem* 2000;**74**:254–62.
31 **Bjartmar C**, Battistuta J, Terada N, *et al.* N-acetylaspartate is an axon-specific marker of mature white matter in vivo: a biochemical and immunohistochemical study on the rat optic nerve. *Ann Neurol* 2002;**51**:51–8.
32 **Litvan I**, Goetz CG, Jankovic J, *et al.* What is accuracy of the clinical diagnosis of multiple system atrophy? *Arch Neurol* 1997;**54**:937–44.
33 **Sparga E**, Papp MI, Lantos PL. Decrease in neuronal density in the cerebral cortex in multiple system atrophy. *Eur J Neurol* 1996;**3**:450–6.
34 **Konagaya M**, Sakai M, Matsuoka Y, *et al.* Multiple system atrophy with remarkable frontal lobe atrophy. *Acta Neuropathol (Berl)* 1999;**97**:423–8.
35 **Matsuo A**, Akiguchi I, Lee GC, *et al.* Myelin degeneration in multiple system atrophy detected by unique antibodies. *Am J Pathol* 1998;**153**:671–6.

Sweet relief for Huntington disease

Masahisa Katsuno, Hiroaki Adachi & Gen Sobue

Oral delivery of a simple, nontoxic sugar molecule alleviates symptoms of Huntington disease in a mouse model (pages 148–154).

A CAG repeat was first pinned to a neurological disorder—spinal and bulbar muscular atrophy (SBMA)—in 1991 (ref. 1). The pathological influence of the affected gene, an androgen receptor, eventually paled beside the growing realization that the repeat itself was key to the disease. A number of other neurological diseases have since been linked to glutamine-encoding CAG repeats, most prominent among them Huntington disease.

Despite the excitement they have sparked, these discoveries have as yet done little to improve the lives of patients, including more than 35,000 with Huntington disease in the United States. In this issue, Tanaka *et al.* move us closer to reaping the benefits of this decade of research. The authors report that in mouse models of Huntington disease, treatment with a nontoxic sugar substance can prevent the development of the brain pathology associated with Huntington disease, and can delay the progress of symptoms such as motor dysfunction. The approach stands out as the most exciting therapeutic prospect to date for Huntington disease, and also holds promise for the entire class of polyglutamine disorders.

In addition to Huntington disease and SBMA, other polyglutamine disorders include several forms of spinocerebellar ataxia, as well as dentatorubral pallidoluysian atrophy[2]. Outside of the polyglutamine stretch, each causative protein seems unrelated, and removal of the causative protein genetically or by other means does not result in disease in humans or animal models[2]. Yet the diseases show phenotypic similarities. The clinical features depend at least partially on the number of CAG repeats, and are influenced by the meiotic instability of the repeat length. These clinical and genetic similarities imply that polyglutamines induce toxicity, although loss of the normal function of causative proteins may influence the disease[3].

Masahisa Katsuno, Hiroaki Adachi and Gen Sobue are in the Department of Neurology, Nagoya University Graduate School of Medicine, Nagoya, 65 Tsurumai-cho, Showa-ku, Nagoya 466-8550, Japan.
e-mail: sobueg@med.nagoya-u.ac.jp

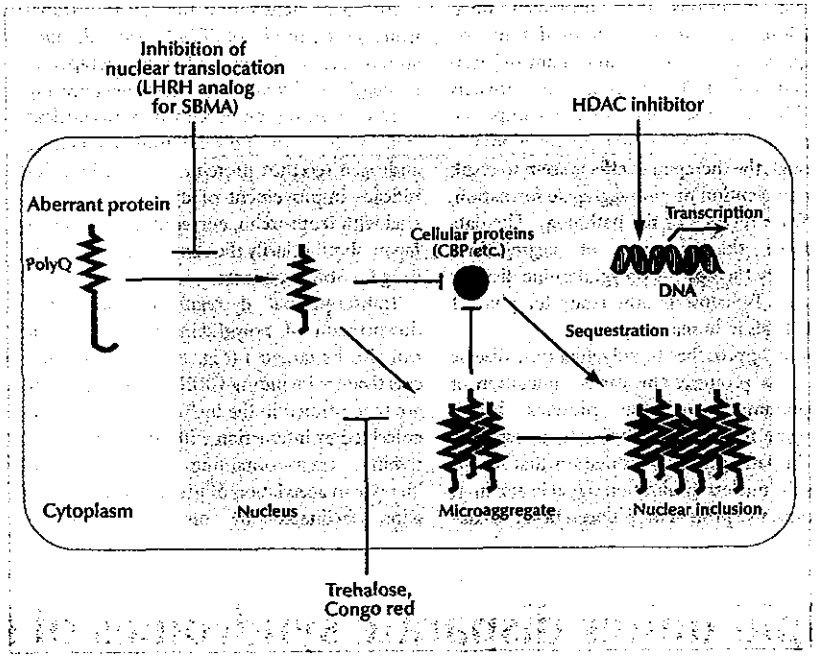

Figure 1 Therapeutic approaches for polyglutamine diseases. Several approaches attempt to mitigate the toxicity of polyglutamine (poly Q) tract–containing proteins. Leuprorelin prevents nuclear uptake of mutant androgen receptor, resulting in the rescue of neuromuscular phenotypes of SBMA. Histone deacetylase inhibitors ameliorate transcription of affected cells. Tanaka *et al.* found that a disaccharide, trehalose, inhibits aggregation of a protein with an expanded polyglutamine tract, especially in the nucleus (as does Congo red). LHRH, luteinizing hormone–releasing hormone; CBP, CREB-binding protein.

How do the glutamine repeats affect the cell? The expansion of the polyglutamine tract alters protein conformation, resulting in the formation of insoluble aggregates. These aggregates sequester normal cellular proteins such as transcription factors, heat shock proteins, ubiquitin, and proteasome components. The propensity of the polyglutamine-containing proteins to aggregate depends on the length of the polyglutamine stretch and is enhanced by protein cleavage through caspase activation.

Patients with polyglutamine diseases show loss of specific types of neurons. The cells that do not die contain inclusions rich in polyglutamine-containing proteins, mainly in the nucleus. These inclusions are found in the vulnerable neurons, implying a direct role in pathogenesis. Whether these aggregates are toxic—a notion supported by a large body of evidence—or reflect a protective response is controversial.

A dramatic study earlier this year bolstered arguments in favor of toxicity. Injection of the dye Congo red prevented formation of nuclear inclusions and alleviated symptoms in a mouse model of Huntington disease[4].

Tanaka *et al.*, favoring the notion that the aggregates are toxic, sought a new aggregation inhibitory therapy for Huntington disease[5]. The authors first used an *in vitro* aggregate formation assay, with myoglobin containing an expanded polyglutamine tract as a target molecule. Using this screening system, they discovered that disaccharides potently inhibited aggregate formation. Trehalose, the most effective disaccharide, selectively stabilized a protein containing a long polyglutamine tract, but not a protein with the normal number of glutamines. The authors confirmed this stabi-

lization in a cell model expressing the aberrant form of huntingtin, the causative protein of Huntington disease. The stabilization of myoglobin with an elongated polyglutamine tract results[6] accounts for the trehalose-mediated suppression of aggregation formation.

The authors went on to test transgenic mouse models of Huntington disease. They found that trehalose-treated mice had fewer nuclear inclusions than untreated mice. Trehalose also improved motor dysfunction and prolonged survival, without any deleterious side effects. The extremely low toxicity and high water-solubility of this compound make this an attractive therapeutic approach, although the therapeutic effects seem to result from prevention of new aggregate formation, not from reversal of the pathology. The data reinforce the rationale of aggregation-inhibitory therapy for polyglutamine diseases (Fig. 1). Trehalose is now ready for phase 1 safety trials in humans.

Other approaches to polyglutamine disease also show promise. Nuclear accumulation of polyglutamine-containing proteins before aggregate formation is probably an essential step in pathogenesis. A mutation that inactivates the nuclear localization signal in ataxin-1, the causative protein in spinocerebellar ataxia-1, nullifies polyglutamine-induced neurodegeneration in a transgenic mouse model[7]. In cell culture, chemically synthesized polyglutamine peptides induce neuronal cell death only when they are directed into the nucleus[8]. These observations suggest that nuclear-directed transport of mutant proteins is an alternative target of intervention (Fig. 1), although cytosolic events should not be neglected[3].

Androgen deprivation therapy in a transgenic mouse model of SBMA clearly demonstrates the usefulness of this therapeutic strategy[9]. A luteinizing hormone–releasing hormone analog, leuprorelin, prevents nuclear translocation of polyglutamine-containing androgen receptor protein, resulting in a significant improvement of disease[9]. A clinical trial with leuprorelin, currently under way in Japan, should clarify the clinical benefit of this drug for SBMA patients.

Transcriptional dysregulation, an event downstream of polyglutamine aggregation, can also be targeted (Fig. 1). Transcriptional coactivators including CREB-binding protein are sequestrated in the inclusion, and are also enfeebled by interaction with soluble polyglutamine tract–containing proteins[3]. An increase in acetylation of nuclear histone proteins, facilitated by histone deacetylase inhibitors, ameliorates neurodegeneration in a mouse model of Huntington disease[10,11]. These compounds have also been used for patients with malignancies. Clinical trials of histone deacetylase inhibitors should be planned carefully, however, taking the hazardous side effects into account.

The promising results of these preclinical studies are ushering in a new era in polyglutamine research: the therapeutic stage. The new investigations also encourage us to continue to search for new, clinically applicable compounds such as aggregation inhibitors. The intensive basic research is bearing fruit, and shows promise of continuing to do so as we move into clinical trials.

1. La Spada, A.R. *et al. Nature* **352**, 77–79 (1991).
2. Zoghbi, H.Y. & Orr, H.T. *Annu. Rev. Neurosci.* **23**, 217–247 (2000).
3. Ross, C.A. *Neuron* **35**, 819–822 (2002).
4. Sanchez, I. *et al. Nature* **421**, 373–379 (2003).
5. Tanaka, M. *et al. Nat. Med.* **10**, 148–154 (2004).
6. Tanaka, M. *et al. J. Biol. Chem.* **276**, 45470–45475 (2001)
7. Klement, I.A. *et al. Cell* **95**, 41–53 (1998).
8. Yang, W. *et al. Hum. Mol. Genet.* **11**, 2905–2911 (2003).
9. Katsuno, M. *et al. Nat. Med.* **9**, 768–773 (2003).
10. Hockly, E. *et al. Proc. Natl. Acad. Sci. USA* **100**, 2041–2046 (2003).
11. Ferrante, R.J. *et al. J. Neurosci.* **23**, 9418–9427 (2003).

Lipid unites disparate syndromes of sepsis

Haichao Wang, Christopher J Czura & Kevin J Tracey

Sepsis is by no means a single clinical entity; physicians must battle a variety of syndromes with only a vague notion of the molecular events that connect them. This vagueness now begins to dissipate with the identification of a molecule that can prevent the development of acute septic shock and severe sepsis (pages 161–167).

In 1347, a mysterious, horrifying disease arrived in Italy and then began to march across the European continent. By the time it reached Sweden three years later, the plague had filled 20 million graves—approximately one-third of the European population. Lacking effective therapeutics, physicians of the time exhaustively defined the signs, symptoms and clinical sequelae of the disease. They determined that patients with 'pestilence' could be readily categorized into two groups with different clinical syndromes. One group developed a slower, more insidious form of the disease, characterized by fever, a roseola rash, flu-like symptoms and enlarged lymph nodes ('buboes'). This 'bubonic' form progressed over 7–14 days, killing 35–70% of its victims. A second group presented with a 'septicemic' form, characterized by acute shock and tissue injury; 80% of these patients died. Until *Yersinia pestis* was identified as the causative agent in the eighteenth century, treatments necessarily targeted clinical signs and symptoms, rather than the underlying source.

In our day, hospitalized patients are dying from severe sepsis, the cause of which is also unknown. It is the most common cause of death in intensive care units, claiming approximately 225,000 victims annually in the U.S. alone. Like their counterparts in fourteenth-century Europe, modern-day physicians carefully describe the clinical signs and symptoms of the syndrome, and focus treatment on the individual complications that develop. After the onset of a bacterial infection, patients can develop distinct clinical syndromes, including acute septic shock and severe sepsis.

In this issue, Yan *et al.*[1] report that administration of a single molecule, lysophosphatidylcholine (LPC), can thwart both syndromes in mouse models. The data begin to reveal a strategy to treat septic shock and severe sepsis, and bring us closer to understanding their underlying causes.

Severe sepsis is defined by signs of systemic

Haichao Wang, Christopher J. Czura and Kevin J. Tracey are at North Shore–LIJ Research Institute, 350 Community Drive, Manhasset, New York 11030, USA. Kevin J. Tracey is a co-founder of Critical Therapeutics Inc., which develops experimental therapies that target critical care medicine.
e-mail: kjtracey@sprynet.com

Neuron, Vol. 41, 677–682, March 4, 2004, Copyright ©2004 by Cell Press

Polyglutamine Diminishes VEGF: Passage to Motor Neuron Death?

Altered gene transcription has been implicated in the pathogenesis of polyglutamine-dependent neurodegeneration. In this issue of *Neuron*, Sopher et al. demonstrate that androgen receptors containing expanded polyglutamine cause decreased expression of vascular endothelial growth factor (VEGF) by interfering with cAMP response element binding protein binding protein (CBP), thereby contributing to the motor neuron degeneration in spinal and bulbar muscular atrophy.

Expansion of a triplet nucleotide repeat is the molecular basis for a variety of hereditary neuromuscular diseases. At least nine neurodegenerative diseases result from a tedious trinucleotide CAG repeat, which encodes a polyglutamine tract (reviewed in Zoghbi and Orr, 2000). These disorders, called polyglutamine diseases, include spinal and bulbar muscular atrophy (SBMA), Huntington's disease (HD), spinocerebellar ataxias (SCA1, 2, 3, 6, 7, and 17), and dentatorubral pallidoluysian atrophy (DRPLA). Several shared clinical and histopathological features seen in polyglutamine diseases imply a common pathogenesis. The patients suffer from slow progressive neuromuscular symptoms with the onset in adulthood. Although the causative genes are distinct, selected subsets of neurons in the central nervous system undergo degeneration in each disease. Histopathological hallmarks are the loss of neurons in the affected area and the existence of characteristic intranuclear inclusions in the residual neuronal cells. These inclusions contain aggregates of the causative protein together with fundamental cellular components, providing a clue to the mechanisms causing neurodegeneration. Although the precise role of these inclusions remains open to debate, a large body of evidence suggests that the nuclear localization of aberrant polyglutamine protein is an essential step in the pathogenesis.

The perturbation of gene transcription is likely to be among the most substantial nuclear events in the pathophysiology of polyglutamine diseases. This hypothesis emerged from the observation that cAMP response element binding protein binding protein (CBP), a transcriptional coactivator, is sequestrated into the polyglutamine inclusion (Nucifora et al., 2001). Furthermore, the acetyltransferase activity of CBP is directly inhibited by the interaction with aberrant polyglutamine protein (Steffan et al., 2001). In agreement with these findings, alteration of a wide range of gene expression has been detected in mouse models of polyglutamine diseases (Sugars and Rubinsztein, 2003). It is of therapeutic significance that polyglutamine-mediated neurodegeneration in a *Drosophila* model of HD is alleviated by histone deacetylase inhibitors, which restore histone acetylation and upregulate gene transcriptions (Steffan et al., 2001). Although decreased transcription appears to be a plausible explanation for the pathogenesis, little direct link between CBP dysfunction and neurodegeneration has been clarified in vivo. In addition, it remains unclear which gene is responsible for neuronal cell death in each polyglutamine disease.

Spinal and bulbar muscular atrophy (SBMA), or Kennedy's disease, which is caused by an expanded CAG repeat in the androgen receptor (AR) gene, was the first disease to be identified as a polyglutamine disease (La Spada et al., 1991). SBMA is an adult-onset lower motor neuron disease characterized by proximal muscle atrophy, weakness, fasciculations, and bulbar involvement. In the central nervous system, the brainstem and the anterior horn are selectively involved. Besides motor neuron degeneration, patients present with several systemic complications: gynecomastia, hyperlipidemia, and glucose intolerance. Since the loss of AR function does not result in neuromuscular phenotypes, the extended polyglutamine tract itself appears to render the causative protein toxic, as documented in other polyglutamine diseases. The disruption of CBP-mediated transcription has also been implicated in the pathogenesis of this disease (McCampbell et al., 2001). Despite a common molecular basis, SBMA is distinct from other polyglutamine diseases in that males are exclusively affected. A transgenic mouse model of SBMA revealed that ligand-dependent nuclear translocation of the pathogenic AR protein accounts for the gender-related pathogenesis, leading to the development of a potential hormonal therapy for this disorder (Katsuno et al., 2002). In this issue of *Neuron*, Sopher et al. (2004) report a new transgenic mouse model carrying human AR yeast artificial chromosome (YAC) with a prolonged CAG repeat. Their study reconfirmed the importance of nuclear accumulation of aberrant AR and ligand-dependent pathophysiology in SBMA. Since the expression of the transgene is controlled by its own promoter, the mRNA level of the mutant AR in this model is less than that in previous mouse models using potent exogenous promoters. This would account for the pathological distribution reminiscent of SBMA and the slow progression of motor disability. Among the conspicuous achievements in this study is the finding that the transgenic mice recapitulate the loss of lower motor neurons in SBMA. Whereas histopathological studies of autopsy cases with polyglutamine diseases show a tangible loss of neurons in lesions, a majority of transgenic mouse models demonstrate neuromuscular disability without detectable cell death (Zoghbi and Orr, 2000). This could be explained by the short life span and excessive expression of the causative polyglutamine protein in these mouse models. Symptomatic phenotypes with normal cell populations may indicate that the pathophysiology of polyglutamine disease rises from the dysfunction of neurons. This hypothesis in turn indicates the reversibility of the pathogenesis at the early stage of the diseases. In support of this view, the interruption of mutant gene

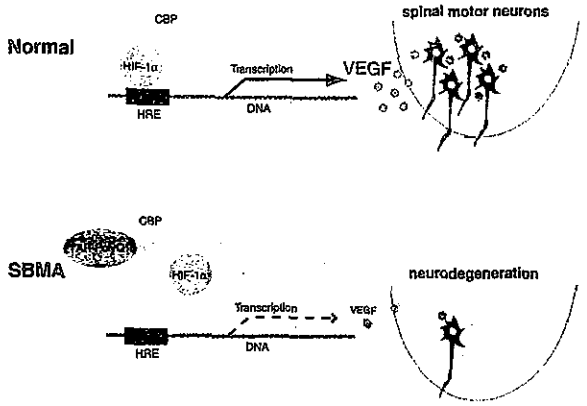

Figure 1. Possible Mechanism of VEGF-Related Motor Neuron Degeneration in SBMA

Hypoxia-inducible factor 1α (HIF-1α) binds to hypoxia-response element (HRE) in the promoter of vascular endothelial growth factor (VEGF), upregulating its transcription. This transactivating activity of HIF-1α is facilitated through interaction with cAMP response element binding protein binding protein (CBP). In spinal and bulbar muscular atrophy (SBMA), the pathogenic androgen receptor (AR) containing expanded polyglutamine (polyQ) interacts with CBP, resulting in decreased level of VEGF. These processes appear to contribute to motor neuron degeneration in SBMA.

expression reversed the symptoms and histopathological features in a conditional mouse model of HD using a tet-regulation system (Yamamoto et al., 2000). Although this observation justifies medical intervention to mildly affected or presymptomatic patients, elucidating the precise mechanism giving rise to neuronal cell death is also essential for the development of therapies for polyglutamine diseases. The study of Sopher et al. appears to offer a striking insight into the pathophysiology of polyglutamine-induced motor neuron death, in their revelation that the interaction between pathogenic AR and CBP results in a reduced expression of vascular endothelial growth factor (VEGF), which appears to contribute to the neurodegeneration in SBMA.

VEGF, first discovered as a factor enhancing vascular permeability, plays a crucial role in physiological and pathological angiogenesis. Diverse biological effects of VEGF are facilitated by its receptor, VEGF-2, also termed kinase insert domain receptor (KDR). The gene expression of VEGF is drastically upregulated upon hypoxia in order to form new blood vessels. Hypoxia-inducible factors, HIF-1α and HIF-2α, mediate this cellular protective response through binding to hypoxia-response element (HRE) in the promoter of VEGF. The transactivating activity of HIF-1α is facilitated through interaction with transcriptional coactivators such as CBP (Figure 1). The depletion of a single allele of VEGF results in embryonic lethality, whereas lack of the HRE sequence in the VEGF promoter leads to slowly progressive motor neuron degeneration (Oosthuyse et al., 2001). Knockin mice harboring a *VEGF* gene in which HRE is deleted demonstrate a late-onset motor neuron disease resembling SBMA and amyotrophic lateral sclerosis (ALS), suggesting a pivotal role for VEGF in neurodegeneration. The low expression level of VEGF in these mice results in loss of spinal motor neurons, axonal degeneration in the peripheral nerve, and neurogenic muscular atrophy, all of which are pathological features of human motor neuron diseases. Moreover, the targeted disruption of HRE results in the marked exacerbation of motor neuron degeneration in transgenic mice carrying mutant superoxide dismutase 1 (SOD 1), the most frequent cause of familial ALS (Lambrechts et al., 2003). The deleterious effects of HRE deletion on motor neurons could be due to the suppression of favorable effects of VEGF: enhancement of blood supply and direct neuroprotection. Given that intraperitoneal administration of VEGF ameliorates ischemia-induced degeneration of spinal motor neurons in the aberrant VEGF knockin mice (Lambrechts et al., 2003), blood circulation insufficiency may cause neuromuscular phenotypes. Since VEGF protects cultured normal motor neurons from apoptotic stimuli, loss of these neurotrophic effects could also contribute to the pathogenesis of motor neuron degeneration due to HRE deletion.

The study of Sopher et al. shows that the reduction in the expression level of VEGF precedes the onset of neurogenic muscular atrophy, suggesting that the transcriptional alteration is a trigger, rather than a consequence, of neurodegeneration. The implication of VEGF in SBMA is also backed by the observation that an exogenous VEGF administration alleviates cytotoxicity induced by pathogenic AR with expanded polyglutamine in their cell model. In addition, CBP cotransfection augments VEGF level in the same cultured motor neurons, implying that the transactivating ability of CBP is suppressed by an aberrant protein-protein interaction with AR. This work sheds light on VEGF as a key player in the pathogenesis of polyglutamine-induced motor neuron degeneration, providing another therapeutic target for SBMA. The retrograde delivery of neurotrophic factors ameliorates neurodegeneration in mouse models of motor neuron diseases to some extent (Kaspar et al., 2003). It should be of value to investigate whether VEGF administration improves the polyglutamine-dependent pathogenesis in the SMBA mouse model of Sopher et al. Alternatively, the repressed transcription of VEGF in SBMA mice suggests that chronic hypoxia aggravates motor neuron degeneration, although its clinical implications have yet to be elucidated. Chronic ischemia, aggravated by lowered level of VEGF, appears to induce oxidative stress, which has been suggested to exacerbate neurodegenerative processes. It thus seems possible that polyglutamine-induced pathophysiology could be ameliorated by antioxidative therapy, which should be tested elsewhere.

A great deal of effort has been made to clarify the exact mechanism causing neuronal dysfunction and the process leading to cell death in polyglutamine diseases. Multiple pathophysiological steps may plunge neurons from dysfunction to death in the presence of an expanded polyglutamine tract. The transcriptional dysregulation of VEGF is likely to play an important role in polyglutamine-induced motor neuron death, since the HRE-deleted mice also showed loss of spinal motor neurons (Oosthuyse et al., 2001). However, whether this hypothesis accounts for the whole pathogenesis of SBMA remains to be resolved. Given that multiple mechanisms are involved in neurodegeneration, we need to clarify which genes, regulated by CBP or other factors,

are responsible for the pathogenesis of polyglutamine diseases. Such clarification would expand therapeutic options for these devastating disorders.

Masahisa Katsuno and Gen Sobue
Department of Neurology
Nagoya University Graduate School of Medicine
Nagoya 466-8550
Japan

Selected Reading

Katsuno, M., Adachi, H., Kume, A., Li, M., Nakagomi, Y., Niwa, H., Sang, C., Kobayashi, Y., Doyu, M., and Sobue, G. (2002). Neuron *35*, 843–854.

Kaspar, B.K., Llado, J., Sherkat, N., Rothstein, J.D., and Gage, F.H. (2003). Science *301*, 839–842.

Lambrechts, D., Storkebaum, E., Morimoto, M., Del-Favero, J., Desmet, F., Marklund, S.L., Wyns, S., Thijs, V., Andersson, J., van Marion, I., et al. (2003). Nat. Genet. *34*, 383–394.

La Spada, A.R., Wilson, E.M., Lubahn, D.B., Harding, A.E., and Fischbeck, K.H. (1991). Nature 352, 77–79.

McCampbell, A., Taye, A.A., Whitty, L., Penney, E., Steffan, J.S., and Fischbeck, K.H. (2001). Proc. Natl. Acad. Sci. USA 98, 15179–15184.

Nucifora, F.C., Jr., Sasaki, M., Peters, M.F., Huang, H., Cooper, J.K., Yamada, M., Takahashi, H., Tsuji, S., Troncoso, J., Dawson, V.L., et al. (2001). Science *291*, 2423–2428.

Oosthuyse, B., Moons, L., Storkebaum, E., Beck, H., Nuyens, D., Brusselmans, K., Van Dorpe, J., Hellings, P., Gorselink, M., Heymans, S., et al. (2001). Nat. Genet. *28*, 131–138.

Sopher, B.L., Thomas, P.S., Jr., LaFevre-Bernt, M.A., Holm, I.E., Wilke, S.A., Ware, C.B., Jin, L.-W., Libby, R.T., Ellerby, L.M., and La Spada, A.R. (2004). Neuron *41*, this issue, 687–699.

Steffan, J.S., Bodai, L., Pallos, J., Poelman, M., McCampbell, A., Apostol, B.L., Kazantsev, A., Schmidt, E., Zhu, Y.Z., Greenwald, M., et al. (2001). Nature *413*, 739–743.

Sugars, K.L., and Rubinsztein, D.C. (2003). Trends Genet. *19*, 233–238.

Yamamoto, A., Lucas, J.J., and Hen, R. (2000). Cell *101*, 57–66.

Zoghbi, H.Y., and Orr, H.T. (2000). Annu. Rev. Neurosci. *23*, 217–247.

Migraine Aura: A Knockin Mouse with a *Knockout* Message

Migraine aura is a sometimes disabling disorder of the brain that involves significant neurological symptoms in about 30% of patients. In this issue of *Neuron*, van den Maagdenberg et al. characterize a mouse with a knockin mutation known to cause familial hemiplegic migraine and provide evidence that a lowered threshold to the triggering of CSD may account for the devastating phenotype of familial hemiplegic migraine.

A good basic neuroscience paper can illustrate a fundamental principle, exploit new methods to open avenues for study, or even point the general direction to the horizon where novel therapies will be found. This issue of the *Neuron* has a contribution that does each of these (van den Maagdenberg et al., 2004). Beginning to model aspects of the most common of the severely disabling forms of primary headache delivers the *knockout* message that common neurobiological problems will yield secrets to basic neuroscience for the ultimate good of patients.

Migraine aura consists of the neurological symptoms, flashing jagged lights, pins and needles, or even weakness, that are so well recognized as preceding the attack proper in about 30% of patients. Familial hemiplegic migraine is a very rare form of migraine with prolonged aura in which an important manifestation is one-sided weakness. So far, from a clinical viewpoint, it has been difficult to dissect its various forms. Mutations in the *CACNA1A* gene that encodes the pore-forming subunit of the P/Q voltage-gated calcium channel ($Ca_V2.1$) cause about 50% of this disorder (Ophoff et al., 1996). In addition, perhaps 30% of patients might be accounted for by mutations in *ATP1A2* gene that encodes the Na^+/K^+ pump α_2 subunit (De Fusco et al., 2003). Both of these changes could lead to increases in intracellular Ca^{2+}, but this has raised the essential "so what" problem: how does this elegant biology enlighten the clinical question, why would this result in episodic, often profound weakness?

Cortical spreading depression is a wave of excitation followed by inhibition that traverses the cortex at a rate of about 3–6 mm/min Pioneering work using human brain blood flow measurements during migraine aura showed that the flow changes associated with aura also moved at this curious slow rate across the brain. Brain imaging (Hadjikhani et al., 2001) has carefully built a case that migraine aura is the human version of the cortical spreading depression measured by electrophysiological methods in experimental animals (Lauritzen, 1994). Studies of migraine aura in humans and cortical spreading depression in experimental animals have led to some very important questions: how is aura triggered in humans, what role might the genetic mutations described above in familial hemiplegic migraine play, and last, what is the role of aura in migraine—is it the pain trigger?

In this issue of *Neuron*, van den Maagdenberg and colleagues report a *Cacna1a* knockin mouse with increased susceptibility to cortical spreading depression. Using the R192Q mutation, which is clearly pathogenic in humans (Ophoff et al., 1996), they very elegantly characterize with electrophysiological methods a gain-of-function in cerebellar granule cells in culture from homozygous mice. At the neuromuscular junction, endplate potentials, used as a measure of acetylcholine-evoked postsynaptic depolarizations, were increased by 240% under conditions of low Ca^{2+} concentration, representing enhanced activation in mutant mice compared to wild-type mice. Using DC potential recordings at the cortex, the authors also noted a lowered threshold for the induction and a remarkable 150% increase in the rate of propagation of cortical spreading depression. Previous work using electrophysiological techniques had shown a gain-of-function at the channel level but a loss-of-function at the whole-cell level in transfected cells that van den Maagdenberg and colleagues attribute to overexpression. A general principle illustrated by the new work is the absolute necessity for whole-animal studies to dissect the effects of mutations and understand the integrated physiology of a disease. Rely-

Journal of Neurochemistry, 2004, **89**, 64–72 doi:10.1046/j.1471-4159.2003.02289.x

Dorfin prevents cell death by reducing mitochondrial localizing mutant superoxide dismutase 1 in a neuronal cell model of familial amyotrophic lateral sclerosis

Hideyuki Takeuchi, Jun-ichi Niwa, Nozomi Hishikawa, Shinsuke Ishigaki, Fumiaki Tanaka, Manabu Doyu and Gen Sobue

Department of Neurology, Nagoya University Graduate School of Medicine, 65 Tsurumai-cho, Showa-ku, Nagoya 466-8550, Japan

Abstract

Dorfin is a RING-finger type ubiquitin ligase for mutant superoxide dismutase 1 (SOD1) that enhances its degradation. Mutant SOD1s cause familial amyotrophic lateral sclerosis (FALS) through the gain of unelucidated toxic properties. We previously showed that the accumulation of mutant SOD1 in the mitochondria triggered the release of cytochrome *c*, followed by the activation of the caspase cascade and induction of neuronal cell death. In the present study, therefore, we investigated whether Dorfin can modulate the level of mutant SOD1 in the mitochondria and subsequent caspase activation. We showed that Dorfin significantly reduced the amount of mutant SOD1 in the mitochondria, the release of cytochrome *c* and the activation of the following caspase cascade, thereby preventing eventual neuronal cell death in a neuronal cell model of FALS. These results suggest that reducing the accumulation of mutant SOD1 in the mitochondria may be a new therapeutic strategy for mutant SOD1-associated FALS, and that Dorfin may play a significant role in this.

Keywords: amyotrophic lateral sclerosis, Dorfin, mitochondria, neuronal cell death, superoxide dismutase 1, ubiquitin ligase.

J. Neurochem. (2004) **89**, 64–72.

Amyotrophic lateral sclerosis (ALS) is a fatal neurodegenerative disease caused by selective death of motor neurons. Approximately 10% of ALS cases are familial (FALS). Missense mutations in the gene coding superoxide dismutase 1 (SOD1) are responsible for approximately 20% of FALS cases (Rosen *et al.* 1993; Hirano 1996) through the gain of unelucidated toxic properties (Yim *et al.* 1996).

Many reports have documented that the mitochondria are involved in the pathogenic process in mutant SOD1-associated FALS. Mitochondrial degeneration, including swelling, dilatation and vacuolization, is an early characteristic pathological feature of FALS and FALS transgenic (Tg) mice models with SOD1 mutations (Dal Canto and Gurney 1994; Wong *et al.* 1995; Hirano 1996; Kong and Xu 1998; Jaarsma *et al.* 2000; Higgins *et al.* 2003). Recently, it was demonstrated that SOD1, considered to be a cytosolic enzyme, exists in the mitochondria (Sturtz *et al.* 2001; Okado-Matsumoto and Fridovich 2001; Higgins *et al.* 2002), and that the mitochondrial vacuoles in mutant SOD1 Tg mice were lined with mutant SOD1 (Jaarsma *et al.* 2001; Higgins *et al.* 2003). Many studies have suggested that the programmed cell death (PCD) pathway contributes to motor neuron death in FALS (Durham *et al.* 1997; Martin 1999; Li *et al.* 2000; Pasinelli *et al.* 2000; Guégan *et al.* 2001; Kriz *et al.* 2002; Raoul *et al.* 2002; Zhu *et al.* 2002). Moreover, we previously reported that accumulation of mutant SOD1 in the mitochondria triggered the release of mitochondrial cytochrome *c*, which subsequently activated the caspase cascade and induced neuronal cell death (Takeuchi *et al.* 2002a). Taken together, these results suggest that the accumulation of mutant SOD1 in the mitochondria is critical in the pathogenesis of mutant SOD1-associated FALS.

Received September 23, 2003; revised manuscript received November 17, 2003; accepted November 24, 2003.

Address correspondence and reprint requests to Gen Sobue, Department of Neurology, Nagoya University Graduate School of Medicine, 65 Tsurumai-cho, Showa-ku, Nagoya 466–8550, Japan.
E-mail: sobueg@med.nagoya-u.ac.jp

Abbreviations used: ALS, amyotrophic lateral sclerosis; COX, cytochrome *c* oxidase; DMEM, Dulbecco's modified Eagle's medium; E3, ubiquitin ligase; EGFP, enhanced green fluorescent protein; FALS, familial amyotrophic lateral sclerosis; MTS, 3-(4,5-dimethyl-thiazol-2yl)-5-(3-carboxymethoxyphenyl)-2-(4-sulfophenyl)-2H-tetrazolium; PCD, programmed cell death; PI, propidium iodide; SOD1, superoxide dismutase 1; Tg, transgenic.

Dorfin is the product of a gene that we cloned from the anterior horn tissue of the human spinal cord (Niwa *et al.* 2001); it contains a RING-finger/IBR motif (Niwa *et al.* 2001) at its N-terminus. It was reported that a distinct subclass of RING-finger/in-between RING-fingers (IBR) motif-containing proteins represents a new ubiquitin ligase (E3) family that interacts specifically with distinct ubiquitin-conjugating enzymes (Moynihan *et al.* 1999; Ardley *et al.* 2001). Dorfin is a juxtanuclearly located E3 that ubiquitylates various SOD1 mutants derived from patients with FALS, and enhances the degradation of mutant SOD1 (Niwa *et al.* 2002). Whether Dorfin can modulate the protein level of mutant SOD1 in the mitochondria, and the subsequent activation of the mitochondrial caspase cascade, is an important and interesting question.

Here we show that Dorfin significantly reduced the amount of mutant SOD1 in mitochondria, the release of cytochrome *c* from mitochondria into the cytosol and the subsequent activation of the caspase cascade, thereby preventing the eventual neuronal cell death in a neuronal cell model of FALS. These results suggest that reducing mutant SOD1 in the mitochondria may be a useful strategy for the treatment of mutant SOD1-associated FALS, and that Dorfin might play a significant role in this.

Materials and methods

Plasmids

Non-organelle-oriented plasmids expressing the enhanced green fluorescent protein (EGFP)-tagged human SOD1 (wild type, mutant G93A, and G85R) were described previously (Takeuchi *et al.* 2002a,b). These vectors express SOD1-EGFP fusion proteins ubiquitously in each organelle (Takeuchi *et al.* 2002a). They were designated Cyto-WT, Cyto-G93A and Cyto-G85R respectively. Mitochondria-oriented plasmids expressing EGFP-tagged human SOD1 (wil dtype, mutant G93A and G85R) with mitochondrial localizing signals were generated as described previously (Takeuchi *et al.* 2002a). These vectors express SOD1-EGFP fusion proteins mainly in the mitochondria (Takeuchi *et al.* 2002a). They were designated Mito-WT, Mito-G93A and Mito-G85R respectively. The plasmid pcDNA3.1/HisMax-Dorfin, which expresses Xpress-tagged Dorfin, was also described previously (Niwa *et al.* 2001). As a control, we used pCMV-β vector expressing LacZ (Clontech, Palo Alto, CA, USA). All constructs used here were confirmed by DNA sequence analysis.

Cell culture

Mouse neuroblastoma cell line Neuro2a cells were maintained in Dulbecco's modified Eagle's medium (DMEM) (Invitrogen Corp., Carlsbad, CA, USA) supplemented with 10% fetal calf serum (Invitrogen Corp.) as described previously (Takeuchi *et al.* 2002b). They were cultured on Laboratory-Tec II four-well chamber slides (Nalge Nunc International, Rochester, NY, USA) coated with poly-L-lysine (Sigma, St Louis, MO, USA). Transient expression of SOD1 plasmids (0.1 μg of DNA/well) and pcDNA3.1/His Max-Dorfin or pCMV-β (0.3 μg of DNA/well) in Neuro2a cells (2×10^4 cells/well) was accomplished with LipofectAMINE PLUS reagent (Invitrogen Corp.). After incubation for 3 h with transfection reagents, transfected cells were cultured in differentiation medium (DMEM supplemented with 1% fetal calf serum and 20 μM retinoic acid). To detect Xpress-Dorfin fusion protein, 0.5 μM proteasome inhibitor MG132 (Sigma) was added 16 h before collection, as described previously (Niwa *et al.* 2001).

Cell fractionation

At each time point (0, 24 and 48 h) after transfection, cells were collected and gently homogenized with a Dounce homogenizer in cold buffer [250 mM sucrose, 10 mM Tris-HCl pH 7.5, 5 mM $MgCl_2$, 2 mM EDTA and protease inhibitor cocktail (Complete Mini EDTA-free; Roche Diagnostics, Basel, Switzerland)]. Cell fractionation was performed as described previously (Takeuchi *et al.* 2002a). To verify the fractionation, each fraction was subjected to western blotting for cytochrome *c* oxidase (COX) as a mitochondrial marker using anti-COX subunit IV mouse monoclonal antibody (1 : 1000; Molecular Probes, Eugene, OR, USA), and β-actin as a cytosolic marker using anti-β-actin mouse monoclonal antibody (1 : 5000; Sigma).

Western blot analysis

The protein concentration was determined with a DC protein assay kit (Bio-Rad Laboratories, Hercules, CA, USA) and western blotting was done as described previously (Takeuchi *et al.* 2002b). To evaluate the level of mitochondrially localized SOD1-EGFP fusion proteins, 20 μg protein from the mitochondrial fraction was loaded. For analyzing the release of cytochrome *c* from the mitochondria into the cytosol, 20 μg protein from the mitochondrial fraction or the cytosolic fraction was loaded.

To assess the levels of SOD1-EGFP fusion proteins, Xpress-Dorfin fusion proteins and the activation of caspase-9 and caspase-3, cells were collected at each time point (0, 24 and 48 h) after transfection, and lysed in TNES buffer (50 mM Tris-HCl pH 7.5, 150 mM NaCl, 1% NP-40, 2 mM EDTA, 0.1% sodium dodecyl sulfate and protease inhibitor cocktail) as described previously (Takeuchi *et al.* 2002a). For the analysis, 20 μg protein from the total lysate was loaded.

The primary antibodies used were as follows: anti-SOD1 rabbit polyclonal antibody (1 : 10 000; StressGen Biotechnologies, Victoria, BC, Canada), anti-Xpress mouse monoclonal antibody (1 : 5000; Invitrogen Corp.), anti-caspase-3 rabbit polyclonal antibody and anti-caspase-9 rabbit polyclonal antibody (1 : 1000; Cell Signaling, Beverly, MA, USA) and anti-cytochrome *c* mouse monoclonal antibody (1 : 1000; Pharmingen, San Diego, CA, USA). After overnight incubation with primary antibodies at 4°C, each blot was probed with horseradish peroxidase-conjugated anti-rabbit IgG and anti-mouse IgG (1 : 5000; Amersham Biosciences, Piscataway, NJ, USA). Blots were then visualized with ECL Plus western blotting detection reagents (Amersham Biosciences). The signal intensity was quantified by densitometry using NIH Image 1.63 software.

Immunocytochemistry

At each time point (0, 24 and 48 h) after transfection, cells were fixed with 4% paraformaldehyde for 30 min on ice and then

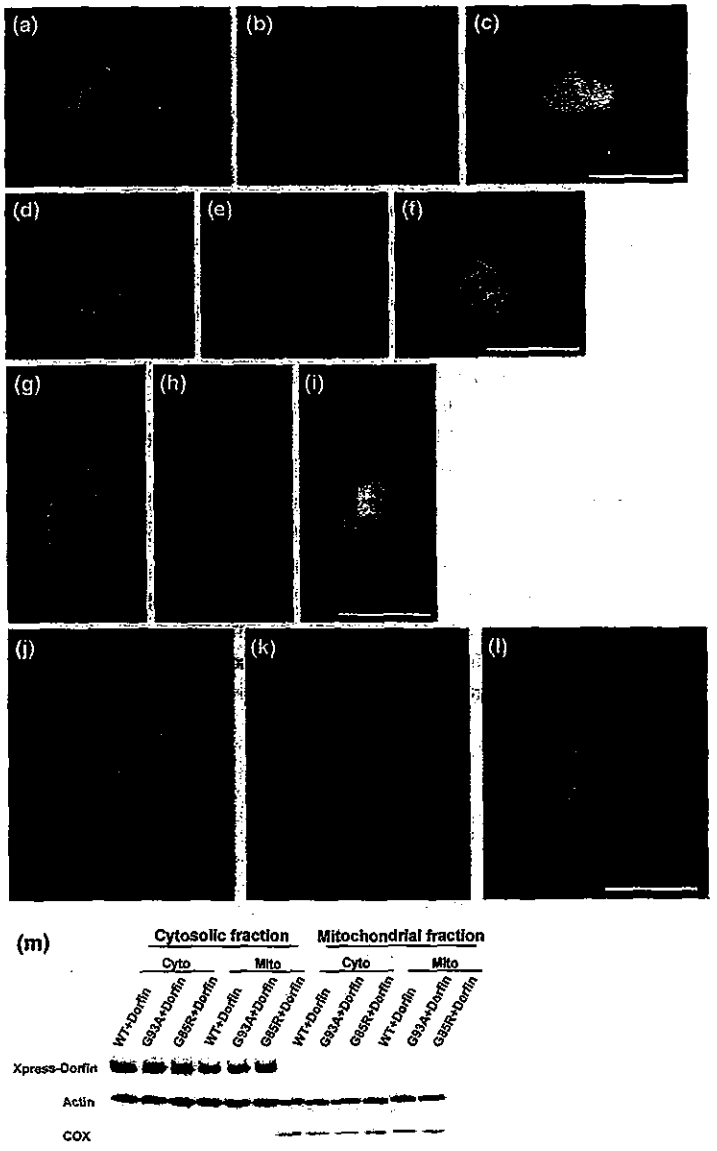

Fig. 1 Subcellular localization of SOD1-EGFP and Xpress-Dorfin in Neuro2a cells. (a–l) Confocal laser scanning microscopic images at 48 h after transfection. (m) Fractionation analysis of Xpress-Dorfin fusion protein. (a–c) Cyto-WT + Xpress-Dorfin, (d–f) Cyto-G93A + Xpress-Dorfin, (g–l) Cyto-G85R + Xpress-Dorfin; (j–l) Mito-G93A + Xpress-Dorfin. SOD1-EGFP fusion proteins (green; a, d and g) and Xpress-Dorfin fusion proteins (red; b, e and h) were observed ubiquitously in the cells with Cyto-SOD1 containing no organelle-oriented signals. SOD1-EGFP fusion proteins and Xpress-Dorfin fusion proteins were co-localized (yellow; c, f and i). In contrast, in the cells with Mito-SOD1, SOD1-EGFP fusion proteins were observed in the mitochondria (green; j) and Xpress-Dorfin fusion proteins (red; k) were observed mainly in the cytoplasm. They were not co-localized in the cells with Mito-SOD1 (l). Cells were counterstained with TO-PRO-3 (blue). Scale bars, 10 μm. Western blots also revealed that Xpress-Dorfin fusion proteins were absent in the mitochondrial fraction (m).

permeabilized with 0.05% Triton X-100 at room temperature for 10 min. They were stained with the anti-Xpress mouse monoclonal antibody (1 : 5000; Invitrogen Corp.) at 4°C overnight. They were subsequently stained with Alexa-568-conjugated secondary antibody (1 : 5000; Molecular Probes) at room temperature for 90 min. Then they were counterstained with 2 μg/mL TO-PRO-3 (Molecular Probes) at room temperature for 10 min, and mounted in Gelvatol. A confocal laser scanning microscope (MRC1024; Bio-Rad Laboratories) was used for the morphological analysis.

Quantitative assessment of mitochondrial impairment and cell death

To assess cell viability through mitochondrial impairment, we used the 3-(4,5-dimethyl-thiazol-2yl)-5-(3-carboxymethoxyphenyl)-2-(4-sulfophenyl)-2H-tetrazolium (MTS) assay with CellTiter 96 Aqueous one solution assay (Promega, Madison, WI, USA), as described previously (Takeuchi *et al.* 2002a). At each time point (0, 24 and 48 h) after transfection, MTS assays were carried out in six independent trials. Absorbance at 490 nm was measured in a multiple plate reader as described previously (Ishigaki *et al.* 2002).

Cell death was assessed by the dye exclusion method with propidium iodide (PI; Molecular Probes) as described previously (Takeuchi *et al.* 2002a). At each time point (0, 24 and 48 h) after transfection, cells were incubated with 2 μg/mL PI in DMEM for 15 min at room temperature and mounted in Gelvatol. More than 200 transfected cells in duplicate slides were assessed blindly in three independent trials under a conventional fluorescent microscope. The ratio of dead cells was calculated as a percentage of PI-positive cells among EGFP-positive cells.

Statistical analysis

All results were analyzed by two-way ANOVA with Tukey–Kramer post-hoc test, using Statview software version 5 (SAS Institute Inc., Cary, NC, USA).